

## A SYSTEMATIC ERROR ANALYSIS OF HP8510 TIME-DOMAIN GATING TECHNIQUES WITH EXPERIMENTAL VERIFICATION

Ke Lu, Thomas J. Brazil

Department of Electronic and Electrical Engineering  
University College Dublin, Dublin 4, Ireland

KK

**ABSTRACT:** The errors caused by using time-domain gating techniques on the HP8510 automatic network analyser are investigated systematically. These errors are divided into four categories: out-of-gate attenuation error, truncation error, masking error and multi-reflection aliasing error. A method to estimate the order of the magnitude errors resulting from time-domain gating is presented. Experiments to support the analysis are designed and carried out, giving results in good agreement with theory.

### I. INTRODUCTION

Following the introduction of a time-domain option onto the HP8510 series of automatic vector network analyser (ANA), time-domain gating techniques have been widely applied for many purposes. Such capabilities are extremely useful when one wishes to extract and isolate a single reflection from a system under measurement which exhibits multiple reflections [1]. Obviously, the use of a time-domain gate in these circumstances could be expected to introduce some errors into the measurement results, but there is very little discussion of this problem in the open literature. There is a need to be able to estimate the resulting errors quantitatively and to establish how these errors affect the final results. In this paper, time-

domain gating errors are systematically divided into four categories and an approximate quantitative error analysis is provided, accompanied by experimental verification. One practical method, which can be used to estimate the order of error magnitudes, is introduced. This contribution aims to identify some basic considerations needed for a systematic and quantitative error analysis applicable to HP8510 time-domain gating techniques.

### II. CLASSIFICATION AND ANALYSIS OF TIME-DOMAIN GATING ERRORS

Figure 1 shows the category of passive systems under consideration in this paper, which it is assumed are to be measured by the ANA. A complete (coaxial) calibration is performed with the ANA up to Port 1 & Port 2. It is assumed that there are several discontinuity points in the system under measurement. These are separated by uniform transmission lines which only introduce small distortions into the measurement results compared with the discontinuity points themselves and can therefore be ignored. When a wide-band frequency measurement is performed on this system, every reflection adds a specific contribution to the frequency response in a quite complex manner to form the final frequency-domain results. If one of these reflections is under special study, the only way to obtain reasonable results directly

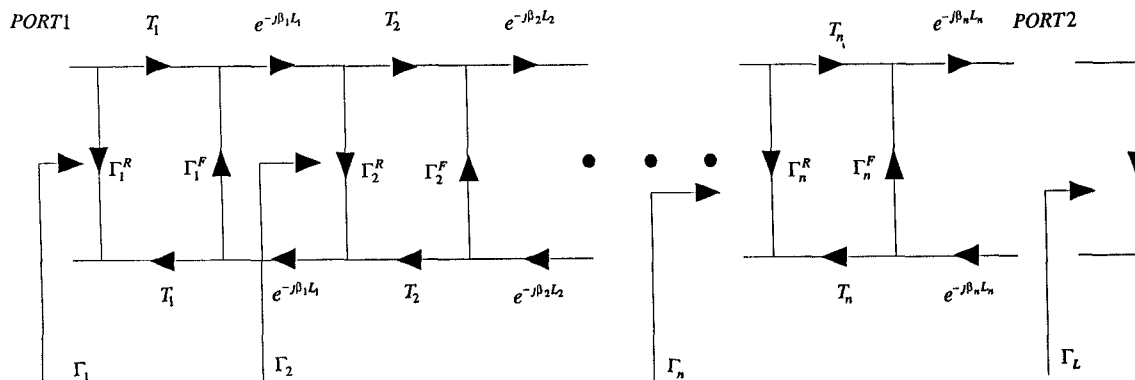


Fig. 1. Typical ANA measurement system setup.

from frequency-domain measurements is by choosing high-quality adaptors and transitions with good performance over a wide frequency range, which only introduce small reflections compared with the reflection under study. Unfortunately, this method often fails because the reflection of interest is small enough to be comparable with the reflections of commercial adaptors or transitions. The time-domain gating technique supplies an option to solve the problem. On the HP8510 for example, through the use of the chirp-Z transform [3], wideband frequency measurement data is translated to the time-domain. The different reflection points, which are separated by uniform transmission structures, are located at different points along the time axis according to their distance from the reference plane. By means of the time-domain gating technique, we can suppress unwanted reflections by putting a window on the reflection under study and gating out other reflections. After the gating operation, the time-domain data is translated to the frequency-domain and the frequency-domain characteristics of the reflection under study are obtained.

Now by inspection of the signal-flow chart shown in Fig.1., the total reflection in the frequency-domain at Port 1 can be obtained as follows [2]:

$$\begin{aligned}
 \Gamma_1 &= \Gamma_1^R + \frac{T_1^2 \Gamma_2 e^{-j2\beta_1 L_1}}{1 - \Gamma_1^F \Gamma_2 e^{-j2\beta_1 L_1}} \\
 \Gamma_2 &= \Gamma_2^R + \frac{T_2^2 \Gamma_3 e^{-j2\beta_2 L_2}}{1 - \Gamma_2^F \Gamma_3 e^{-j2\beta_2 L_2}} \\
 &\vdots \\
 \Gamma_i &= \Gamma_i^R + \frac{T_i^2 \Gamma_{i+1} e^{-j2\beta_i L_i}}{1 - \Gamma_i^F \Gamma_{i+1} e^{-j2\beta_i L_i}} \\
 &\vdots \\
 \Gamma_n &= \Gamma_n^R + \frac{T_n^2 \Gamma_L e^{-j2\beta_n L_n}}{1 - \Gamma_n^F \Gamma_L e^{-j2\beta_n L_n}}
 \end{aligned} \tag{1}$$

Expression (1) can be expanded as follows:

$$\begin{aligned}
 \Gamma_1 &= \Gamma_1^R + T_1^2 \Gamma_2^R e^{-j2\beta_1 L_1} + T_1^2 T_2^2 \Gamma_3^R e^{-j2(\beta_1 L_1 + \beta_2 L_2)} + \\
 &\quad T_1^2 T_2^2 T_3^2 \Gamma_4^R e^{-j2(\beta_1 L_1 + \beta_2 L_2 + \beta_3 L_3)} + \dots + T_1^2 (\Gamma_2^R)^2 \Gamma_1^F e^{-j4\beta_1 L_1} + \\
 &\quad T_1^2 T_2^2 (\Gamma_3^R)^2 \Gamma_2^F e^{-j2(\beta_1 L_1 + 2\beta_2 L_2)} + \dots + T_1^2 (\Gamma_2^R)^4 (\Gamma_1^F)^2 e^{-j6\beta_1 L_1} + \dots \\
 &= R_1(f) + R_2(f) + \dots + R_m(f) + \dots
 \end{aligned} \tag{2}$$

where  $\beta_i$ ,  $L_i$  are the propagation coefficient and length of  $i$ -th transmission line section,  $T_i$ ,  $\Gamma_i^F$ , and  $\Gamma_i^R$  are S-parameters of the  $i$ -th discontinuity point, where  $S_{11}^i = \Gamma_i^R$ ,  $S_{22}^i = \Gamma_i^F$ , and  $S_{21}^i = S_{12}^i = T_i$ ,.  $R_m(f)$  is the  $m$ -th term

Typical time-domain waveform for multi-reflection system on HP8510 network analyser

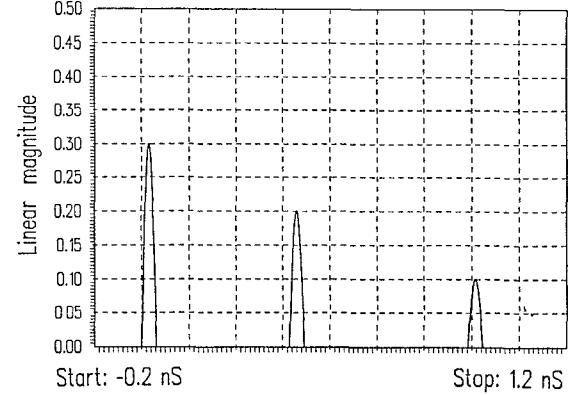


Fig. 2. Time-domain waveform of a triple-reflection system

determined by rearranging different terms according to the cumulative value of the exponential term index. In the time-domain technique used in the HP8510, Eq. (1) is directly transformed to the time-domain using the chirp-Z transform. In the time-domain, the overall system reflection  $\Gamma_1(t)$  then appears like many reflection peaks distributed along the time-axis, as illustrated in Fig. 2:

$$\Gamma_1(t) = r_1(t) + r_2(t) + \dots + r_m(t) + \dots$$

$$r_i(t) = \int_{-\infty}^{\infty} R_i(f) e^{j\omega t} d\omega \tag{3}$$

where  $r_i(t)$  is the (causal)  $i$ -th reflection peak located at  $t_i$ , and an integral Fourier Transform representation has been used for convenience. In the case of the HP8510, a chirp-Z transform is actually applied to transform measurement data between time and frequency domain. This technique represents a compromise between FFT and DFT in terms of execution time and flexibility. Now, let us assume that the first reflection  $r_1(t)$  is under study or, in terms of the frequency domain, this means the function  $\Gamma_1^R(\omega)$ . The time-domain gating technique can be used to extract  $\Gamma_1^R(\omega)$  from  $\Gamma_1(\omega)$ . The gating function used in the HP8510 is shown in Fig.3. To simplify the analysis, we use the following two-value function to approximate the gate function in HP8510:

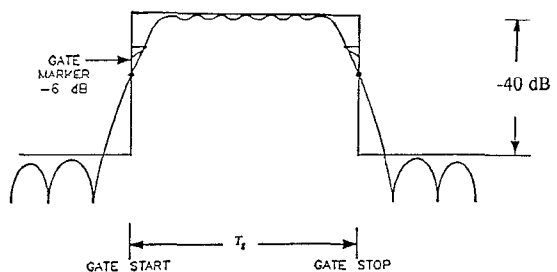


Fig. 3. Gate characteristics of HP8510 and two value approximation.

$$g(t) = \begin{cases} 1 & t_{start} < t < t_{stop} \\ K & \text{otherwise} \end{cases} \quad (4)$$

Suppose that  $T_g$  is selected as the gate width. After the gating operation, and when the result is transformed to the frequency-domain, we obtain:

$$\begin{aligned} \Gamma_{1,gate}^{1-st}(\omega) &= \int_0^{T_g} r_1(t) e^{-j\omega t} dt + K \int_{T_g}^{\infty} r_1(t) e^{-j\omega t} dt + K \sum_{i=2}^{\infty} \int_{T_g}^{\infty} r_i(t) e^{-j\omega t} dt \\ &= \Gamma_1^R(\omega) + E1(\omega) + E2(\omega) \end{aligned} \quad (5)$$

where  $\Gamma_{1,gate}^{1-st}(\omega)$  represents the frequency-domain reflection coefficient following gating on  $r_1(t)$ . So there are two kinds of errors in this measurement:

#### Out-of-Gate Attenuation Error

$$E1(\omega) = K \int_0^{\infty} \sum_{i=2}^{\infty} r_i(t) e^{-j\omega t} dt \quad (6)$$

where  $K$  is quoted as -40dB or 0.01 for the HP8510. This error is caused by incompletely suppressing the reflections outside the range of the gate.

#### Truncation Error

$$E2(\omega) = (K-1) \int_{T_g}^{\infty} r_1(t) e^{-j\omega t} dt \quad (7)$$

This situation arises, for example, when a long duration response has applied to it a time-width-limited gate, thereby losing the tail of the response and causing a *truncation error*. Even when the gate is applied to the other reflections the above two errors still exist and the equations (5)-(7) have a similar form for such cases.

#### Masking Error

In the situation where the *second* reflection is under study, we find that application of the time-domain gate leads, in the frequency-domain, to:

$$\begin{aligned} \Gamma_1^{2-nd}(\omega) &= T_1^2(\omega) \Gamma_2^R(\omega) + E1(\omega) + E2(\omega) \\ &= E3(\omega) \Gamma_2^R(\omega) + E1(\omega) + E2(\omega) \end{aligned} \quad (8)$$

$E3$  is described here as the *Masking Error* and represents the fact that the measurement results are influenced by the transmission coefficients of discontinuity points prior to the reflection under study.

#### Multi-Reflection Aliasing Error

When the *third* reflection is under study, a new error term could arise if the system being measured consists of commensurate lines ( $\beta_1 L_1 = \beta_2 L_2$ , etc.):

$$\begin{aligned} \Gamma_1^{3-nd}(\omega) &= T_1^2(\omega) T_2^2(\omega) \Gamma_3^R(\omega) + T_1^2(\omega) (\Gamma_2^R(\omega))^2 \Gamma_1^F(\omega) + \\ &\quad + E1(\omega) + E2(\omega) \\ &= E3(\omega) \Gamma_3^R(\omega) + E4(\omega) + E1(\omega) + E2(\omega) \end{aligned} \quad (9)$$

In this case,  $E4$  is the multi-reflection response that arrives the input at the same time as does the first reflection from  $\Gamma_3^R(\omega)$ . This is described here as the *Multi-Reflection Aliasing Error*.

Normally, when a reflection is extracted by a gating operation, the gating error of the reflection measurement is the combination of the above four kinds of error. If all the  $L_i$ 's are long enough to separate the discontinuity points, the error term  $E2$  can be ignored. The contribution of  $E4$  is normally one- or two- orders of magnitude less than  $E1$  due to the high-order small term  $(\Gamma_i^R(\omega))^2$  and the non-commensurate condition, thus the effect of  $E4$  is usually negligible. Hence, the predominant contribution to the time-domain gating error generally comes from the terms  $E1$  and  $E3$ .

### III. ERROR ESTIMATE FOR HP8510 TIME-DOMAIN GATING TECHNIQUES

Equations (1)-(9) would be useful to estimate the time-domain gating error if the reflection and transmission coefficients of the unwanted discontinuities have been given or could be estimated roughly. This is true for most transitions or adaptors, but for many cases the reflection or transmission coefficients of the unwanted discontinuities are not available in advance. In the following we introduce a simple method which is useful where the unwanted discontinuities are lossless or low loss and reciprocal.

According to [1], for the time-domain option as implemented on the HP8510, the linear magnitude value of the reflection peak in the time-domain can be interpreted as the average reflection coefficient of the discontinuity over the frequency range of the measurement. Let us consider as a specific example, a triple-reflection system with three reflection peaks in the time-domain, as depicted in Fig.2. The values of the peaks are 0.3, 0.2, 0.1, respectively, corresponding to frequency-domain functions  $\Gamma_1^R, T_1^2 \Gamma_2^R$ , and  $T_1^2 T_2^2 \Gamma_3^R$ . Hence,

according to Eq. (1) and assuming ( $|T_1^2| = 1 - |\Gamma_1^2|$  and  $|T_2^2| = 1 - |\Gamma_2^2|$ ):

$$\begin{aligned}\Gamma_{1,gate}^{1-st} &= \Gamma_1^R + KT_1^2\Gamma_2^R + KT_1^2T_2^2\Gamma_3^R \\ &\approx \Gamma_1^R \pm 0.01[0.2 + 0.1] \\ &\approx 0.3 \pm 0.003\end{aligned}$$

This means that using time-domain gating, approximately 1% error could be expected in the estimate of the linear magnitude. Also, in the case of the second reflection:

$$\begin{aligned}\Gamma_{1,gate}^{2-nd} &= KT_1^R + T_1^2\Gamma_2^R + KT_1^2T_2^2\Gamma_3^R \\ &\approx \Gamma_2^R - 0.09\Gamma_2^R \pm 0.004\end{aligned}$$

so that about a 12% error could be expected. Similarly, for the third reflection a 20% error may be estimated. It is seen therefore, that using Eq. (1) it is very easy to obtain the order of the error arising from gating operations. Several additional points should be mentioned:

- (1) This method gives an approximate estimate of the error based on average reflection coefficients;
- (2) The error distribution is nonuniform across the frequency range due to the frequency-dependent characteristics of the system. At some points, such as for example, an absorbing peak, the relative error could be very large due to the small reflection at those points.

A complete experimental verification of this approach is rendered very difficult by the intrinsic complexity of the problem. However, for the simple system represented in Fig. 4., we have devised a simple but effective method of experimental verification. In Fig. 4. there is a system in which say the first reflection is under study (this reflection is actually realised using a small removable reflection block on a microstrip line). Following the first reflection there is a section of uniform transmission line and then the load end. We firstly perform the full two-port calibration of this system to Port 2 and without introducing first discontinuity. Then the discontinuity point is introduced to the system ( $\Gamma_1^R, \Gamma_1^F, T_1$  ). In this case  $E_1$  is negligible due to the fact that  $\Gamma_L = 0$ , so the measurement gives a *true reflection coefficient* for the first discontinuity. Then a short circuit is added to the load end. The time-domain gate is used to gate out the (large) second reflection to obtain the first reflection coefficient with error  $E_1$ . Then, by comparing the *true reflection coefficient* and the reflection coefficient with gating error, the error  $E_1$  of the gating technique is obtained for this case. By using (5) and the true reflection coefficient of the first discontinuity point, the  $E_1$  term can be calculated at every frequency point. Comparing with the error predicted by (5), good agreement is obtained, as seen in Fig. 5, where the theoretical prediction and the real measurement relative error are both presented.

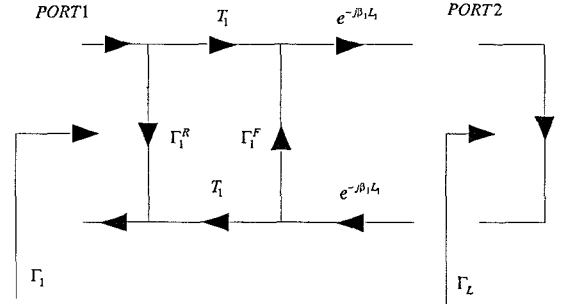


Fig. 4. A simple two-reflection system

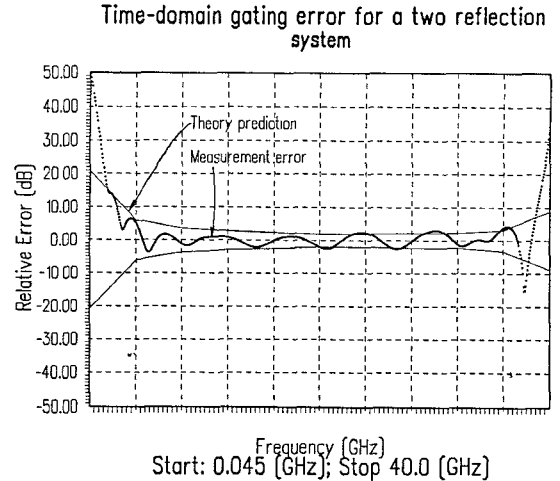


Fig. 5. Comparing theory predicted error and true error

#### IV. CONCLUSION

A novel error analysis for HP8510-based time-domain gating techniques is introduced. A method is given by which the order of the magnitude errors can be roughly estimated, and the approach has been validated in an experimental example. This work should be useful to help create confidence in measurement results obtained from time-domain gating techniques on vector network analysers.

#### REFERENCES

- [1] Hewlett-Packard: "HP8510C User's Manual."
- [2] Qizheng Gu, J. A. Kong: " Transient analysis of single and coupled lines with capacitively-loaded junctions" IEEE Trans. MTT, No.9., p952, 1986
- [3] B. Ulriksson, " Conversion of frequency-domain data to the time domain" Proc. IEEE, Vol. 74, No.1, pp. 74-77, 1986.